





Review

Singlet Oxygen in Photodynamic Therapy

Shengdong Cui ¹, Xingran Guo ¹, Sen Wang ¹, Zhe Wei ¹, Deliang Huang ¹, Xianzeng Zhang ¹, Timothy C. Zhu ² 
and Zheng Huang ^{1,*} 

¹ MOE Key Laboratory of Medical Optoelectronics Science and Technology, Key Laboratory of Photonics Technology of Fujian Province, School of Optoelectronics and Information Engineering, Fujian Normal University, Fuzhou 350117, China

² Department of Radiation Oncology, University of Pennsylvania, Philadelphia, PA 19104, USA

* Correspondence: zheng_huang@msn.com

Abstract: Photodynamic therapy (PDT) is a therapeutic modality that depends on the interaction of light, photosensitizers, and oxygen. The photon absorption and energy transfer process can lead to the Type II photochemical reaction of the photosensitizer and the production of singlet oxygen ($^1\text{O}_2$), which strongly oxidizes and reacts with biomolecules, ultimately causing oxidative damage to the target cells. Therefore, $^1\text{O}_2$ is regarded as the key photocytotoxic species accountable for the initial photodynamic reactions for Type II photosensitizers. This article will provide a comprehensive review of $^1\text{O}_2$ properties, $^1\text{O}_2$ production, and $^1\text{O}_2$ detection in the PDT process. The available $^1\text{O}_2$ data of regulatory-approved photosensitizing drugs will also be discussed.

Keywords: singlet oxygen; photodynamic therapy; photosensitizer; detection methods



Citation: Cui, S.; Guo, X.; Wang, S.; Wei, Z.; Huang, D.; Zhang, X.; Zhu, T.C.; Huang, Z. Singlet Oxygen in Photodynamic Therapy.

Pharmaceuticals **2024**, *17*, 1274.

<https://doi.org/10.3390/ph17101274>

Academic Editor: Céline Frochot

Received: 30 July 2024

Revised: 10 September 2024

Accepted: 10 September 2024

Published: 26 September 2024



Copyright: © 2024 by the authors. Licensee MDPI, Basel, Switzerland. This article is an open access article distributed under the terms and conditions of the Creative Commons Attribution (CC BY) license (<https://creativecommons.org/licenses/by/4.0/>).

1. Introduction

Photodynamic therapy (PDT) is a modern therapeutic technology that depends on the interdisciplinary integration of pharmaceuticals, optics, and medicine. PDT has been used to treat various benign and malignant diseases [1]. The therapeutic responses of PDT depend on the interaction of light, photosensitizers (PSs), and molecular oxygen within the target cells and tissues [2]. In general, PDT involves two main steps: the topical or systemic administration of photosensitizing drugs and light irradiation of the treatment site accumulated with the PS. In the presence of molecular oxygen, this process leads to the generation of reactive oxygen species (ROS) and, particularly, the photosensitized formation of singlet oxygen ($^1\text{O}_2$), the key photophysical step in Type II photosensitization. The initial biological responses and effectiveness of PDT treatment are ultimately determined by the temporal and spatial distribution of $^1\text{O}_2$.

Photosensitizers commonly employed in clinical practice can be classified into groups such as porphyrins, chlorins, or other dyes from the chemist's point of view. Porphyrins are a widely used PS, which include Porphimer Sodium, PhotoGem, and Hiporfin [3], also known as hematoporphyrin derivative (HpD), which is the complex mixture of water-soluble porphyrin monomers and oligomers that are purified from animal blood [4]. Aminolevulinic acid (ALA) and its ester derivatives are prodrugs that are metabolized in cells and enzymatically converted to protoporphyrin IX (PpIX), a potent endogenous porphyrin type PS [5]. Chlorin-type PSs used in clinical practice includes Temoporfin (m-THPC) and Laserphyrin (LS11) [6,7]. Phthalocyanines and organic dyes, for instance, aluminum phthalocyanine tetrasulfonate (ALPcS4), usually have long absorption wavelengths and high extinction coefficients [8].

Most PSs exhibit PDT effects primarily characterized by the Type II photochemical reaction and the efficient production of $^1\text{O}_2$ [9]. $^1\text{O}_2$ strongly oxidizes and reacts with biomolecules. The mechanism of $^1\text{O}_2$ -mediated PDT highly depends on the subcellular localization of the PS and the oxidative destruction of organelles, such as mitochondria,

lysosomes, endoplasmic reticulum, Golgi apparatus, and plasma membranes. When exceeding the cell's antioxidation capacity, the acute oxidative stress to these organelles can induce changes in calcium and lipid metabolism, the production of cytokines and stress proteins, and the activation of protein kinases and transcription factors. These cellular responses can ultimately lead to apoptosis and necrosis of targeted eukaryotic cells and prokaryotic cells. Subsequently, $^1\text{O}_2$ -generated cytotoxicity exerts a distinctive therapeutic mechanism of the direct killing of target cells, damaging blood vessels, and inducing an immune effect [10]. Therefore, $^1\text{O}_2$ is regarded as the key photocytotoxic species accountable for the initial tissue damage during PDT. The triplet sensitization in the PDT process is a very effective way to generate $^1\text{O}_2$, which makes $^1\text{O}_2$ -mediated PDT a powerful treatment modality with unique mechanisms and broad clinical applications [11]. This article provides a comprehensive review focusing on the $^1\text{O}_2$ production from a clinically used PS based on the recent literature.

2. Properties of Singlet Oxygen

2.1. Electronic Structure and Leaps in Singlet Oxygen

According to the molecular orbital theory, the two highest energy electrons of triplet-state oxygen should be filled in two π -antibonding orbitals and spin-parallel, respectively. It has two unpaired electrons; thus it is paramagnetic. This oxygen molecule with unpaired electrons is triplet-state oxygen, symbolized as $^3\text{O}_2$ ($^3\Sigma_g^-$) [12]. Figure 1 illustrates the three lowest electronic state energy level transitions and molecular orbital schematics of oxygen molecules. When the $^3\text{O}_2$ becomes excited, the two electrons with opposite spins and the highest energy can be arranged in two ways: (1) The two electrons with opposite spins occupy a single π orbital simultaneously, and the other orbital is the empty orbital, which is the first excited singlet state of the oxygen molecule, i.e., singlet oxygen, symbolized as $^1\text{O}_2$ ($^1\Delta_g$). (2) The two electrons with opposite spins each occupy two π orbitals, which is the second excited singlet state oxygen molecule, symbolized as $^1\text{O}_2$ ($^1\Sigma_g^+$) [13]. The three forms of the oxygen molecule are called spin isomers: $^3\text{O}_2$ ($^3\Sigma_g^-$), $^1\text{O}_2$ ($^1\Delta_g$), and $^1\text{O}_2$ ($^1\Sigma_g^+$). The energy difference between $^1\text{O}_2$ ($^1\Sigma_g^+$) and $^1\text{O}_2$ ($^1\Delta_g$) is 0.56 eV, while the energy difference between $^1\text{O}_2$ ($^1\Delta_g$) and $^3\text{O}_2$ ($^3\Sigma_g^-$) is 0.98 eV [14]. The decay of $^1\text{O}_2$ ($^1\Sigma_g^+$) to $^1\text{O}_2$ ($^1\Delta_g$) by the internal conversion process is fast, while $^1\text{O}_2$ ($^1\Delta_g$) to $^3\text{O}_2$ ($^3\Sigma_g^-$) is a slower process. So, in general, singlet oxygen refers to the $^1\text{O}_2$ ($^1\Delta_g$) state [13].

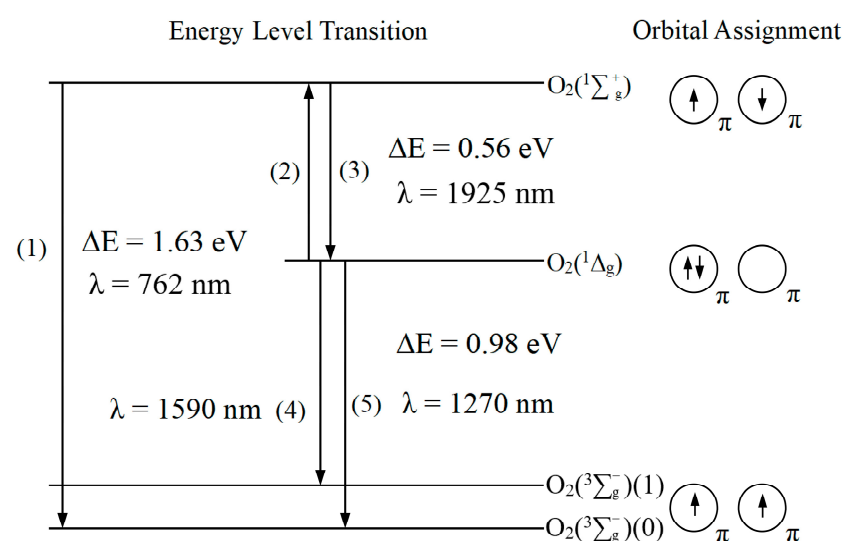


Figure 1. The lowest electronic state energy level transitions and molecular orbital schematics of the oxygen molecule. The configuration of the molecular orbitals of the $^1\Delta_g$ can be described as follows: $\text{O}_2\text{KK}(2\sigma_g)^2(2\sigma_u)^2(3\sigma_g)^2(1\pi_u)^4(1\pi_g^+)(1\pi_g^+)$.

Salokhiddinov et al. report that the radioluminescence intensity of transition (5) ($\lambda = 1270$ nm) is 60 times higher than that of transition (4) ($\lambda = 1590$ nm), based on the detection of the $^1\text{O}_2$ luminescence signal of mesoporphyrin IX dimethyl ester dissolved in carbon tetrachloride (CCl_4) using a highly sensitive germanium diode detector [15]. Macpherson et al. report that the radioluminescence intensity of transition (5) is 100 times higher than that of transition (4), based on the study of the $^1\text{O}_2$ luminescence signals of 5,10,15,20-tetra(4-sulfonato) phenylporphine (TTPS), 5,10,15,20-tetrakis (pentafluorophenyl) porphine (TPPF), and 5,10,15,20-tetraphenylporphine (TTP) in different solutions (e.g., methanol, toluene, CCl_4 , etc.) [16].

Since the energy (ΔE) of $^1\text{O}_2$ ($^1\Delta_g$) is 0.98 eV higher than that of $^3\text{O}_2$ ($^3\Sigma_g^-$), the difference in excitation energy from the S_0 to the S_1 and the difference in energy transfer from the T_1 to the S_0 of the PS should be higher than 0.98 eV, which is a necessary but not sufficient condition for the production of $^1\text{O}_2$ by the PS. Spiller et al. suggest that the excitation energy difference of S_0 to S_1 (see Figure 2) is 1.85 eV for phthalocyanine zinc(II) (ZnPc) and 1.63 eV for 1,4,8,11,15,18,22,25-octa (hexyloxy) phthalocyanine zinc(II) (ZnOHP), respectively [17]. Darwent et al. suggest that the T_1 to S_0 energy transfer differences for 2,9,16,23-tetrasulfophthalocyanine zinc(II) (ZnPc) and 5,10,15,20-tetraphenyl porphyrin zinc(II) (ZnTPP) are 1.12 eV and 1.59 eV, respectively [18].

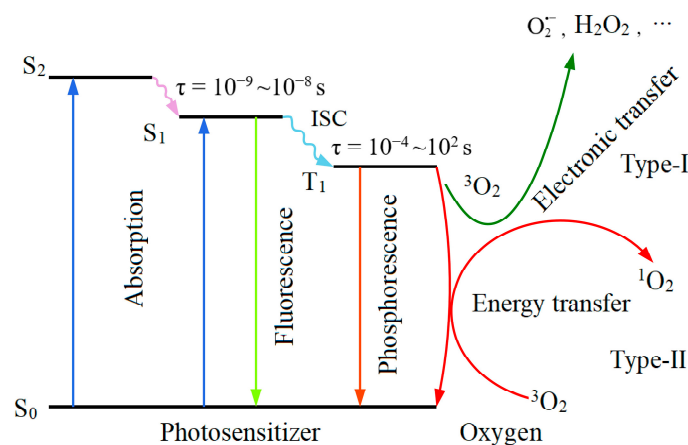


Figure 2. Simplified Jablonski energy level diagram of Type I and Type II photochemical reaction.

2.2. Physical Chemistry Properties of Singlet Oxygen

Without reacting with the surrounding molecules, $^1\text{O}_2$ can return to the ground state and emit photons through spontaneous radiation transition, known as $^1\text{O}_2$ luminescence (or phosphorescence), corresponding the wavelength (λ) of an emission peak near 1270 nm [19]. But not all $^1\text{O}_2$ produced emits light through spontaneous radiation. The luminescence rate constant (k_e) for $^1\text{O}_2$ is the rate at which $^1\text{O}_2$ is consumed by the luminescence process upon return to the ground state. The k_e of $^1\text{O}_2$ varies in different solvents, e.g., the k_e of $^1\text{O}_2$ in water is 0.25 s^{-1} [20]. The intrinsic lifetime of $^1\text{O}_2$ refers to its lifetime in an ideal state without undergoing any chemical reactions, and it is described by $\tau_\Delta = 1/k_e$. τ_Δ is dependent on the properties of molecular structure and energy level. In experimental conditions, the lifetimes of $^1\text{O}_2$ can vary in different solutions, cellular environments, or biological environments. Table 1 lists the lifetimes of $^1\text{O}_2$ in different solvents.

The lifetime of $^1\text{O}_2$ is mainly determined by the quenching rate constant (k_q), which falls under two categories: physical and chemical. Physical quenching involves energy transfer without a chemical reaction. In this process, $^1\text{O}_2$ interacts with a quenching agent and transfers its energy to heat or other forms of energy before returning to $^3\text{O}_2$. For instance, excited singlet-state β -carotene can transfer energy to $^1\text{O}_2$, producing triplet-state β -carotene and $^3\text{O}_2$, therefore, effectively quenching 250~1000 molecules of $^1\text{O}_2$ [21]. The chemical quenching process involves a reaction in which a chemical reacts with the quencher to create a new compound, and ultimately leads to a change in the chemical struc-

ture of the quencher or even results in quencher depletion. For example, $^1\text{O}_2$ reacts with amines to produce free radicals and ascorbate to form hydrogen peroxide (H_2O_2) [21,22]. The quenching effect reduces the concentration of $^1\text{O}_2$. The rate of quenching depends on the stereoelectronic structure of the quencher molecule. For example, C-H, N-H, and O-H groups can quickly transfer vibrational energy, a non-radiative transition process, and can distribute the excited molecular energy through the vibrational modes within the molecule, thus speeding up the quenching process [21]. The quenching rate directly impacts the lifetime of $^1\text{O}_2$. A fast quenching process shortens the lifetime, whereas a slow process or low quencher concentration prolongs it. The k_q , k_e , and τ_Δ of porphyrins are listed in Table 1.

Table 1. The quenching rate constant, luminescence rate constant, and lifetime of $^1\text{O}_2$ in different solvents.

Solvent	k_q ($\text{M}^{-1}\text{s}^{-1}$)	k_e ($\text{M}^{-1}\text{s}^{-1}$)	τ_Δ (μs)
H_2O	2.9×10^9 ^a	0.25 ^b	3.1 ^{a,b,c}
CH_3OH	1.2×10^9 ^c	0.81 ^b	9.5 ^a
C_6H_{14}	5.5×10^8 ^a	N/A	23.4 ^a
C_6H_6	3.9×10^8 ^a	4.5 ^b	30 ^a
C_5H_{12}	4.5×10^8 ^a	N/A	34.7 ^a
D_2O	3.7×10^8 ^a	0.22 ^b	68 ^{a,b}
CD_3OD	N/A	0.79 ^b	270 ^b

^a: data from [23]; ^b: data from [20]; and ^c: data from [24]. N/A: not available.

Quenching can be achieved by adding a quenching agent, which is now mostly used to verify the existence of $^1\text{O}_2$. The use of sodium azide (NaN_3) in an aqueous solution at a concentration greater than 9 mM can quench $^1\text{O}_2$, and adding deuterium oxide (D_2O) possibly also extends the lifetime of $^1\text{O}_2$ to make detection easier. Table 2 summarizes the k_q and the quenching mode of several commonly used $^1\text{O}_2$ quenchers.

Table 2. Quenching rate constant and quenching mode of commonly used $^1\text{O}_2$ quenchers.

Photosensitizer	Quencher	Solvent	k_q ($\text{M}^{-1}\text{s}^{-1}$)	Type of Quenching	Reference
Chlorophyll	β -Carotene ($\text{C}_{40}\text{H}_{56}$)	Benzene Methanol	1.3×10^{10} 9.3×10^9	Physical Physical	[25]
Rose Bengal and Eosin Y	Sodium azide (NaN_3)	Water	6×10^8	Physical	[26]
2-Acetonaphthone	Vitamin E (α -Tocopherol)	Methanol Toluene	3×10^8 2.2×10^8	Physical Physical	[27]
Rose Bengal and Porphyrin	Histidine ($\text{C}_6\text{H}_9\text{N}_3\text{O}_2$)	Water	4.6×10^7	Physical and Chemical	[28]
Rose Bengal and Porphyrin	Tryptophan	Water	3.2×10^7	Physical and Chemical	[28]
Methylene Blue	Tyrosine	water	7×10^6	Chemical	[29]

Cells contain various biomolecules, including lipids, proteins, and nucleic acids. These biomolecules can react rapidly with $^1\text{O}_2$ and cause quenching. Lipids play essential roles as a fundamental part of the cell membrane, a source of energy storage, and as an intermediary in various signaling processes. The reaction of $^1\text{O}_2$ with the free and esterified forms of unsaturated fatty acids in lipid molecules mainly involves para-reactions, resulting in isomeric allylic hydroperoxides. $^1\text{O}_2$ also reacts with cholesterol to produce cholesterol

aldehydes [30]. $^1\text{O}_2$ reacts with several amino acid residues in proteins (e.g., histidine, tryptophan, and tyrosine) in a reaction that is essentially a chemical quenching of $^1\text{O}_2$. Therefore, $^1\text{O}_2$ has a short lifetime and limited diffusion distance within the cell. Moan et al. demonstrate that the average diffusion distance of $^1\text{O}_2$ in the cellular environment is 100–150 nm, and it is 20 nm intracellularly with the $^1\text{O}_2$ lifetime of 40 ns in the skin and liver of living rats [31]. Ethirajan et al. suggest that the diffusion distance of $^1\text{O}_2$ in the cellular environment is only 45 nm, as the lifetimes in the lipid and cytoplasmic regions of the cell membrane are 100 ns and 250 ns, respectively [32]. These data suggest that $^1\text{O}_2$ cannot penetrate through the cellular membrane.

2.3. Oxidizing Activity of Singlet Oxygen

The oxidizing capacity can be measured by its standard redox potential. The standard redox potential of $^1\text{O}_2$ is 2.23 V, which is 1 V higher than that of $^3\text{O}_2$ [33]. H_2O_2 , a Type I ROS, is also a strong oxidizer with a standard redox potential of 1.77 V [34]. Although H_2O_2 is a two-electron strong oxidizer, it exhibits minimal or no interaction with the majority of biomolecules, including low molecular weight antioxidants (e.g., vitamin E and vitamin C) [35]. The presence of a pair of electrons with opposite spins in the highest occupied molecular orbital confers dienophile features to $^1\text{O}_2$. $^1\text{O}_2$ readily reacts with unsaturated organic compounds by electrophilic addition and electron extraction [13]. It can also react with free radicals through energy transfer or electron transfer. In certain chemical reactions, $^1\text{O}_2$ can transfer energy to other molecules, resulting in the creation of free radicals. For instance, $^1\text{O}_2$ reacts with unsaturated fatty acids in cell membranes, leading to the formation of hydroperoxides through Alder-ene reactions with linoleic and linolenic acids, and ultimately causing lipid peroxidation [36]. The oxidation of amino acid residues in proteins by $^1\text{O}_2$ (e.g., the oxidation of methionine residues to sulfoxides, oxidation of histidine to hydroxyimidazolone, and oxidation of tryptophan to N-formylkynurenine) leads to protein structural changes and function loss [37,38]. $^1\text{O}_2$ can also react with lipids or thiols via electron transfer, leading to free radical formation [39,40]. $^1\text{O}_2$ also induces the oxidation of guanine and causes oxidative damage of DNA [41]. These reactions and the high redox potential suggest that the oxidizing power of $^1\text{O}_2$ is stronger than H_2O_2 . However, the decomposition of H_2O_2 creates super-oxidizing hydroxyl radicals ($\bullet\text{OH}$) with an oxidation potential of 2.8 V, making them potent oxidizing ROS produced in the PDT process [42]. This can also be reflected by the difference between the wide ranges of the half-life of different ROS. For instance, the half-life of $^1\text{O}_2$ ranges between 10^{-9} and 10^{-6} s, and that of $\bullet\text{OH}$ between 10^{-9} and 10^{-7} s [43].

Antioxidants are substances that, when present in low concentrations compared to those of an oxidizable substrate, significantly inhibit or prevent the oxidation of that substrate. They act as reducing agents, donating electrons to neutralize free radicals, thereby preventing the formation of oxidative chain reactions that can damage cells and lead to various diseases and conditions [44]. An imbalance between oxidants and antioxidants in a biological system favors oxidants, which can lead to damage known as oxidative stress [45]. Both light-dependent and light-independent processes in biological systems may produce $^1\text{O}_2$. The light-independent reactions include those catalyzed by peroxidases or oxygenases, and reactions of H_2O_2 with hypochlorite (ClO^-) or nitrite. Additionally, the recombination of peroxy radicals ($\text{ROO}\bullet$) derived from biomolecules can lead to the release of $^1\text{O}_2$ [30]. Additionally, light-dependent processes undergo photosensitization to generate $^1\text{O}_2$. Experimental evidence has directly or indirectly suggested that the following naturally occurring ROS are major ones causing oxidative damage in the human body: superoxide radical anion ($\text{O}_2^{\bullet-}$), H_2O_2 , $\text{ROO}\bullet$, $\bullet\text{OH}$, $^1\text{O}_2$, and peroxynitrite (ONOO^-) [46]. To counteract the assault of these ROS, living cells have a biological defense system composed of enzymatic antioxidants that convert ROS to harmless species. For example, $\text{O}_2^{\bullet-}$ can be converted to $^3\text{O}_2$ and H_2O_2 by superoxide dismutase, and H_2O_2 can be converted to water and $^3\text{O}_2$ [46]. In contrast, some ROS are dependent on quenching by various non-enzymatic antioxidants. Non-enzymatic endogenous antioxidants include lipid-based

antioxidants (e.g., carotenoids and vitamin E) and water-soluble antioxidants (e.g., vitamin C, glutathione, and hemoglobin) [47].

Excess $^1\text{O}_2$ in biological systems can destroy cells or tissues, potentially causing irreversible oxidative damage, carcinogenesis, and promoting tumor survival. When the antioxidant system is dysregulated, such as through the overexpression of glutamate–cysteine ligase and glutamate–cysteine catalytic subunit, it can lead to an imbalance in the glutathione/glutathione disulfide ratio [48], generating an excess of $^1\text{O}_2$. This imbalance can disrupt the integrity of biomolecules, cause cellular damage, generate oxidative stress, and damage mitochondria and DNA, ultimately leading to apoptosis, necrosis, senescence, and a proliferation blockade [49].

Physiological levels of $^1\text{O}_2$ have signaling roles within the cell and may act as modulators of cell signaling [49]. It exerts a significant influence on cellular activities, usually with reversibly oxidized hydrogen sulfide groups as signaling molecules to maintain a dynamic equilibrium of generated and quenched $^1\text{O}_2$. The amount of $^1\text{O}_2$ in an organism is regulated by various factors, including the physiological state and environmental conditions. Nevertheless, it is difficult to define a high or low level of $^1\text{O}_2$ as a specific value.

3. Singlet Oxygen Production in PDT Process

PDT is a two-step procedure: (1) the patient is first topically or systemically given a PS (“photosensitizing drug”) that preferentially accumulates in the target tissue, and (2) the light of a specific wavelength generated by a laser light source, LED light source, or daylight is then applied to the treatment site in order to activate the PS. The process of PDT to produce $^1\text{O}_2$ involves the interaction of PS molecules with light irradiation in the presence of molecular oxygen. Therefore, the PS, light, and oxygen are considered as the three crucial elements of PDT. The process of $^1\text{O}_2$ production includes photon absorption, emission, and energy transfer as the PS undergoes different electronic states to eventually generate an excited triplet-state PS and convert the absorbed light energy to highly cytotoxic $^1\text{O}_2$. PSs used in PDT are usually conjugated unsaturated organic molecules that possess high light absorption coefficients, high intersystem crossing efficiencies, and high quantum yields for the production of $^1\text{O}_2$ or other ROS [50].

When the PS is exposed to the light of a specific wavelength and absorbs photon energy, PS molecules in the ground state (S_0) are transitioned to an energy level above the first excited singlet state (S_1). Subsequently, the PS molecules in the S_1 will undergo vibrational relaxation and either decay to the lowest vibrational energy level of that electronic state or decay through internal conversion and vibrational relaxation to the lowest energy level of S_1 .

The lifetime of S_1 is short (10^{-8} – 10^{-9} s) due to the rapid rate of internal transitions [51]. Therefore, the observed luminescence of an S_1 radiation, accompanied by the S_1 to S_0 radiative transitions, is called fluorescence. PS molecules in the S_1 undergo intersystem crossing (ISC) through non-radiative transitions from the S_1 to the slightly lower energy excited triplet state (T_1). The emission of light resulting from the transition from the T_1 to S_0 is known as phosphorescence. This process is spin-forbidden, leading to a low rate constant, with a lifetime ranging from 10^{-4} to 10^2 s for the T_1 [51].

Because the S_1 of the PS molecule has a much shorter lifetime than the T_1 , the likelihood of energy transfer with $^3\text{O}_2$ is reduced. The T_1 -state PS, with its longer lifetime, can effectively transfer energy to $^3\text{O}_2$, leading to the formation of $^1\text{O}_2$. A simplified Jablonski energy level diagram for the Type I and Type II photochemical reactions in the PDT process is shown in Figure 2.

The concentration of $^1\text{O}_2$ generated during PDT is a crucial factor in determining the therapeutic effect, and its concentration is related to many factors and can be expressed as the following:

$$[^1\text{O}_2](t) = N\delta[S_0]\Phi_\Delta \frac{\tau_\Delta}{\tau_T - \tau_\Delta} \left[\exp\left(-\frac{t}{\tau_T}\right) - \exp\left(-\frac{t}{\tau_\Delta}\right) \right] \quad (1)$$

where $[^1\text{O}_2]$ represents the concentration of $^1\text{O}_2$ at time t , N is the number of photons during the excitation pulse, δ the absorption cross-section of the PS, $[S_0]$ is the concentration of the ground-state PS, Φ_Δ is the quantum yield of $^1\text{O}_2$, τ_T is the lifetime of the PS in its triplet state, and τ_Δ is the lifetime of $^1\text{O}_2$.

4. Singlet Oxygen Detection

4.1. Direct Detection of Singlet Oxygen

Detection methods for $^1\text{O}_2$ are broadly categorized into direct and indirect methods. The direct detection of $^1\text{O}_2$ luminescence is considered the “gold standard” for PDT dosimetry. $^1\text{O}_2$ is directly detected by measuring its luminescence at 1270 nm [52]. The long wavelength and low energy of $^1\text{O}_2$, along with its low emission probability in biological media (approximately 10^{-8}), contribute to its inactivation through collision with water molecules under physiological conditions. This results in a short lifetime of $^1\text{O}_2$ on solvents or biological environments, rendering its accurate detection exceedingly arduous using direct detection methods. Therefore, near-infrared photodetectors based on high sensitivity, when integrated with time-resolved counting techniques (e.g., gated photon counting, multichannel counting, and time-correlated single-photon counting), have emerged as a pivotal method for the direct detection of $^1\text{O}_2$ lifetimes. Currently, high-sensitivity NIR detectors for the direct detection of $^1\text{O}_2$ luminescence include the photomultiplier tube (PMT) [53], InGaAs/InP single photon avalanche diode (SPAD) [54], and superconducting nanowire single photon detector (SNSPD) [55,56].

4.2. Indirect Detection of Singlet Oxygen

4.2.1. Electron Paramagnetic Resonance

The electron paramagnetic resonance (EPR) method detects $^1\text{O}_2$ by utilizing the change in the EPR signal after the EPR spin-trapping agent interacts with the $^1\text{O}_2$. The method can determine the yield of $^1\text{O}_2$ by detecting the change in the EPR signal. EPR has a high degree of sensitivity and selectivity in the detection of $^1\text{O}_2$, but it is susceptible to the interference of solvents and coexisting ions. In 1976, McIntosh and Bolton combined the phenomenon of chemically induced dynamic electron polarization with changes in the rate of free radical generation to specifically detect the production of $^1\text{O}_2$ as low as 100 nM [57]. Many researchers have tried to improve the EPR method for the study of $^1\text{O}_2$. For instance, to study the $^1\text{O}_2$ quenching effect of hydroxyl radicals in the presence of thioredoxin by using 2,2,6,6-tetramethyl-4-piperidine (TMP) as a trapping agent [58]. However, EPR spectroscopy is not ideal for detecting intracellular $^1\text{O}_2$, given that its temporal resolution typically spans from microseconds to milliseconds, whereas the lifetime of $^1\text{O}_2$ within cells is usually in the nanosecond scale [12].

4.2.2. Fluorescence Photometry

Fluorescent probes are characterized by high sensitivity, simple data acquisition, high imaging resolution, etc., and are excellent sensors for detecting $^1\text{O}_2$ [59]. By detecting changes in fluorescence properties (fluorescence at specific wavelengths, changes in fluorescence signal intensity, fluorescence quantum yield, etc.), it is possible to determine whether or not $^1\text{O}_2$ is produced. Commonly used organic fluorescent probes mainly include probes with fluorescent signals of their own, which have a significant change in fluorescent signal intensity after $^1\text{O}_2$ is captured, and probes that do not have fluorescent signals of their own, but will generate strong fluorescent signal after $^1\text{O}_2$ is captured. The fluorescence probe includes 1,3-Diphenylisobenzofuran (DPBF) [60], 9-[2-(3-Carboxy-9,10-diphenyl)anyhryl]-6-hydroxy-3H-xanthen-3-ones (DPAXs) [61], and 9-[2-(3-carboxy-9,10-dimethyl)anyhryl]-6-hydroxy-3H-xanthen-3-one (DMAX) [62]. DMAX reacts faster with $^1\text{O}_2$ and is 53 times more sensitive than DPAXs. While DPBF ($9.6 \times 10^8 \text{ M}^{-1}\text{s}^{-1}$) exhibits a higher rate constant for its reaction with $^1\text{O}_2$ in water environments compared to DMAX ($9.1 \times 10^8 \text{ M}^{-1}\text{s}^{-1}$), its reactivity with ClO^- and hydroxyl radicals diminishes its selectivity as a probe for $^1\text{O}_2$.

detection [63]. These probes react with $^1\text{O}_2$ to form stable endoperoxides. They have been used to detect $^1\text{O}_2$ in neutral or alkaline aqueous solutions.

The singlet oxygen green sensor (SOSG) is a fluorescent probe for in vitro detection that is highly selective for $^1\text{O}_2$ [64]. To apply the fluorescent probe to biological samples, the fluorescent probe needs to penetrate the cell membrane and localize inside the cell to directly react with the $^1\text{O}_2$ molecules. Recently, 9,10-dimethylanthracene (DMA) and silicon-containing rhodamine (Si-rhodamine) moieties, a far-red fluorescent probe namely Si-DMA, have been developed to detect $^1\text{O}_2$ in the mitochondria. Murotomi et al. demonstrated that Si-DMA can quantitatively measure intracellular $^1\text{O}_2$ in living cells [65].

4.2.3. Spectrophotometry

Spectrophotometry utilizes an absorption probe to detect $^1\text{O}_2$, where the absorbance value changes upon capture of the $^1\text{O}_2$ and the difference in absorbance is used to express the amount of $^1\text{O}_2$ produced. Spectrophotometry is a relatively simple method for the detection of $^1\text{O}_2$, and the commonly used absorption probes include 9,10-anthracenedipropionic acid (ADPA) [66] and 9,10-diphenyl anthracene (DPA) [67]. Some probes can dissolve in water and undergo irreversible reactions with $^1\text{O}_2$, leading to the creation of stable endoperoxides. For instance, ADPA reacts with $^1\text{O}_2$ to produce endoperoxides, with a peak photobleaching absorption occurring at around 378 nm [68]. Absorption probes enable real-time visualization and monitoring of $^1\text{O}_2$, providing a useful tool for exploring the generation, distribution, and dynamics of $^1\text{O}_2$ in biological environments.

4.2.4. Chemiluminescence

Fluorescence photometry and spectrophotometry are based on the reaction of probe molecules with $^1\text{O}_2$, which results in a significant increase in fluorescence or a decrease in absorbance. On the other hand, chemiluminescence does not require an excitation light source and can directly eliminate the interference of background light, making it a suitable method for detecting $^1\text{O}_2$. When the chemical probe reacts with $^1\text{O}_2$, it produces highly energetic compounds, which are usually unstable and release energy during photolysis. The presence or absence of $^1\text{O}_2$ is determined by detecting light at a specific wavelength. Some common chemical probes include 2-methyl-6-phenyl-3,7-dihydroimidazo[1,2- α]pyrazine-3-one (CLA) [69] and its derivatives, such as 4,4'-(5')-bis[2-(9-anthryloxy)ethylthio]tetra-fulvalene (TTF). In the $\text{H}_2\text{O}_2/\text{ClO}^-$ system, the sensitivity of the detection of $^1\text{O}_2$ is as low as 76 nM [70].

5. Available Singlet Oxygen Data of Regulatory-Approved PS

Quantum yield is an important parameter that measures the ability of a PS to produce $^1\text{O}_2$. It is crucial to accurately determine the $^1\text{O}_2$ quantum yield of a particular PS in various media. When an excited PS is quenched by $^3\text{O}_2$, it produces $^1\text{O}_2$. The efficiency of this process is referred to as the $^1\text{O}_2$ quantum yield (Φ_Δ), which is the ratio between the number of $^1\text{O}_2$ produced and the number of photons absorbed by the PS.

$$\Phi_\Delta = \frac{\text{number of singlet oxygen generated}}{\text{number of photons absorbed}} \quad (2)$$

The Φ_Δ of a PS is an inherent characteristic that varies depending on the molecular structure and photophysical properties of the PS. Accurately quantifying the Φ_Δ of a Type II PS is important for evaluating PDT effectiveness [71].

Oxygen depletion is an indirect technique to accurately measure the Φ_Δ by dissolving the PS in a solvent and passing oxygen through the solution utilizing a gas pump to ensure a steady supply of dissolved oxygen during the reaction. Oxygen consumption is accurately measured under steady-state irradiation conditions using gas microtubes; it is a process that requires sufficient substrate to quantitatively capture and intercept all $^1\text{O}_2$ produced during the photoreaction. The Φ_Δ can be determined from the ratio between the number of moles of oxygen consumed and the number of einsteins absorbed by the PS [72]. Lysozyme

inactivation can be used as an indirect method for measuring the Φ_{Δ} . When $^1\text{O}_2$ reacts with lysozyme, it leads to the inactivation of lysozyme, and this inactivation is proportional to the concentration of $^1\text{O}_2$. The production of $^1\text{O}_2$ can be determined by measuring the activity of the remaining lysozyme. The Φ_{Δ} can be calculated by comparing the difference between lysozyme and lysozyme-free activities [73]. In addition, the excited-state PS is a common precursor of $\text{O}_2^{\bullet-}$ and $^1\text{O}_2$. The $\text{O}_2^{\bullet-}$ reacts with cytochrome C, leading to a cytochrome C reduction. This process can be measured by checking the production of $\text{O}_2^{\bullet-}$ and the number of photons absorbed by the PS, which helps calculate the quantum yield of $\text{O}_2^{\bullet-}$. The production of $^1\text{O}_2$ also depends on the number of photons absorbed by the PS. Thus, the Φ_{Δ} can be indirectly determined by comparing the relative yields of $\text{O}_2^{\bullet-}$ and $^1\text{O}_2$ [74].

The time-resolved infrared luminescence (TRIL) method can also be used to directly detect the Φ_{Δ} generated by a PS. First, the absorption spectrum of the PS is recorded using a spectrophotometer to determine the absorption coefficient. Then, the luminescence intensity of $^1\text{O}_2$ is directly detected using a PMT. By measuring the number of photons absorbed by the PS and the luminescence intensity of $^1\text{O}_2$ the Φ_{Δ} can be calculate [75]. These methods are often calibrated using the quantum yield of a reference PS. The most commonly used calibration PSs are Rose Bengal (RB: $\Phi_{\Delta} = 0.75$) and Methylene Blue (MB: $\Phi_{\Delta} = 0.52$) [75]; Pheophorbide-a is also used as a calibration reference by some researchers [17]. Table 3 provides a summary of the methods used for the determination of quantum yield and specific values for several regulatory-approved PSs for clinical applications. It should be noted that many direct and indirect measurements are often carried out in deuterated solvents, which can improve $^1\text{O}_2$ detection but might increase experiment costs and complications depending upon the required solvent [75,76].

Table 3. Characterization of photosensitizer approved for PDT.

Photosensitizer	λ_{max} (nm)/ ϵ_{max} ($\text{M}^{-1}\text{cm}^{-1}$)	Solvent/(Standard)	Φ_{Δ}	Method	Reference
Porfimer Sodium	632/3000	PBS/TX100 (RB:0.75)	0.89	Lysozyme inactivation	[73]
Hematoporphyrin derivative (HpD)	630	Methanol	0.64	Oxygen depletion	[77]
		Methanol-D	0.76	Oxygen depletion	[72]
Protoporphyrin IX (PpIX)	630/3480	D-PBS/TX100 (RB:0.75)	0.78	TRIL	[75]
		PBS/TX100 (RB:0.75)	0.8	TRIL	[75]
		PBS/TX100 (MB:0.52)	0.56	Lysozyme inactivation	[73]
Meta-tetra(hydroxyl phenyl) chlorin (m-THPC)	652/35,000	Ethanol (Pheophorbide-a:0.52)	0.42	TRIL	[78]
N-aspartyl chlorin e6 (NPe6)	664/40,000	D ₂ O (RB:0.75)	0.66	Oxygen depletion	[79]
		PBS (MB:0.52)	0.64	Lysozyme inactivation	[80]
Benzoporphyrin derivative monoacid ring A (BPD-MA)	689/34,000	Ethanol	0.81	Cytochrome C reduction	[74]
		Methanol	0.78	Cytochrome C reduction	[74]
		Benzene	0.77	TRIL	[80]
Talaporfin sodium (mono-L-aspartyl chlorine e6)	654/40,000	D-PBS (RB:0.75)	0.53	TRIL	[75]
		D-PBS/TX100 (RB:0.75)	0.59	TRIL	[73]
Aluminum phthalocyanine tetrasulfonate (ALPcS4)	676/200,000	PBS/TX100	0.38	Lysozyme inactivation	[73]

Based on Table 3, it is evident that various PSs exhibit unique optical properties. The maximum absorption wavelengths (λ_{max}) and molar extinction coefficients (\mathcal{E}_{max}) of these PSs can impact their light absorption efficiency and tissue penetration depth, thereby influencing the effectiveness of PDT. The development and design of new PSs of different chemical, biological, and optical properties continue to be the focus of PDT research.

The extinction coefficient (\mathcal{E}) quantifies how efficiently a PS absorbs light at a specific wavelength (λ). The subscript “max” denotes the peak extinction coefficient (\mathcal{E}_{max}) and peak absorption wavelength (λ_{max}), respectively. The penetration depth of light in a target tissue depends on the scattering and absorption properties of the tissue at the specific wavelength of the light [81]. The actual “phototherapeutic window” of PDT ranges between 600 nm and 800 nm [82]. The λ_{max} and \mathcal{E}_{max} of porphyrin PSs are relatively low compared with those of other types of PSs. For example, Photofrin[®], the drug form of Porfimer Sodium, has an \mathcal{E}_{max} of 3000 M^{−1}cm^{−1} at 630 nm, while ALPcS4 has an \mathcal{E}_{max} of 200,000 M^{−1}cm^{−1} at 676 nm [73]. The low \mathcal{E}_{max} value of the PS at λ_{max} indicates that the PS absorbs light weakly at the λ_{max} . Generally speaking, the larger the \mathcal{E}_{max} value, the higher potential PDT response. However, in contrast, the lower \mathcal{E}_{max} value of a certain PS does not necessarily correlate to a reduced Φ_{Δ} . For instance, Photofrin[®] and ALScP4 exhibit Φ_{Δ} of 0.89 and 0.38 in phosphate buffer saline (PBS) (pH 7.4) in the presence of 1 vol% Triton X-100 (PBS/TX100), demonstrating a complex interplay between PS’s absorption optical properties, energy transfer, and efficacy in generating ¹O₂ [73]. Numerous studies demonstrate that non-halogenated and halogenated BODIPYs (4,4-difluoro-4-bora-3a,4a-diaza-s-indacene) have very similar λ_{max} values, but very different Φ_{Δ} values, suggesting no absolute correlation between Φ_{Δ} and λ_{max} [83].

The Φ_{Δ} of the PS is influenced not only by their inherent structure but also by the measurement technique, ambient environmental conditions, and excitation wavelength. The Φ_{Δ} for the same PS, measured under consistent conditions, may differ by measurement methods (e.g., the Φ_{Δ} values for PpIX in PBS/TX100 solution are 0.8 and 0.56 when measured using TRIL and Lysozyme inactivation methods, respectively) [73,75]. The Φ_{Δ} for a PS measured by the same method can also vary under different environmental conditions. For example, using the oxygen depletion method, the Φ_{Δ} values for HpD in methanol and methanol-D solutions are 0.64 and 0.76, respectively [72,77]. Using the TRIL method, the Φ_{Δ} values for Talaporfin sodium in Dulbecco’s PBS (D-PBS) and D-PBS/TX100 solutions are 0.53 and 0.59, respectively [73,75]. Even when the same method is used to measure the Φ_{Δ} for the same PS under the same solution conditions, there may be some differences. This could be related to the polarity of the solvent, ionic strength, or the interactions between the PS and solvent molecules.

In clinical applications, the λ_{max} , \mathcal{E}_{max} , and Φ_{Δ} of the PS can be used as the main criteria for selecting a particular PS. Factors such as the metabolism time of the PS in the body, the duration of the skin photosensitivity response, and the selectivity to the diseased tissue also affect the PDT effect. Porphyrin-type PSs are the most extensively studied, but they have longer skin photosensitivity durations and a lower selectivity for diseased tissues. For instance, Porfimer Sodium, which is purified from HpD, requires a higher drug/light dose during treatment and necessitates 4 to 6 weeks of light avoidance after treatment [84]. Chlorin PSs are widely used clinically due to their strong photosensitivity, high target specificity, and minimal side effects. For example, NPe6 hardly participates in metabolic processes in the body, offering better safety [85]. Phthalocyanine PSs have strong absorption in the “phototherapeutic window”, but they exhibit very low or no absorption in the spectrum of sunlight (400~600 nm), thereby reducing the degree of skin photosensitivity [86]. Nevertheless, the selection and use of PSs also require a comprehensive consideration of these properties, pharmacological and therapeutic strategies, and their impact on therapeutic efficacy and patient safety to achieve optimal PDT outcomes [87,88].

6. Conclusive Remarks

Singlet oxygen is molecular oxygen in the excited state and widely exists in nature. The fundamental properties of $^1\text{O}_2$ have been well documented. It is well-known that $^1\text{O}_2$ can react with simple organic molecules, complex biological molecules, and cellular components with high-rate constants. $^1\text{O}_2$ could be generated via various processes. However, triplet sensitization is a very effective way to generate the lowest excited singlet state of oxygen. The term “ $^1\text{O}_2$ ” usually refers to the lowest energy excited species ($^1\Delta_g$) of molecular oxygen. Triplet states of PS molecules under illumination can undergo energy transfer with oxygen molecules in the $^3\Sigma_g^+$ state, facilitating the ISC process from the triplet to singlet states of O_2 , producing $^1\text{O}_2$. By understanding and utilizing $^1\text{O}_2$ reactivity, it has been possible to develop unique therapeutic tools that can be precisely employed for destructive purposes via $^1\text{O}_2$ -mediated oxidative damages, for example, the medical applications of the photoinduced production of $^1\text{O}_2$ in PDT.

Ever since Photofrin[®] was officially approved as the first PDT PS drug for the treatment of superficial and solid cancers, the development of new non-toxic PS dyes has been focused on improving PDT efficacy, shortening cutaneous photosensitivity, and expanding indications worldwide. Several PSs have received regulatory approval over the past three decades globally. Currently, PDT mediated by these traditional PSs has been used topically and systemically for the treatment of various cancer, pre-cancer, vascular, and infectious diseases. It should be recognized that each PS has its advantages and disadvantages. Nonetheless, the Type II mechanism and the production of $^1\text{O}_2$ are regarded as the fundamental process in current PDT protocols. PSs should ideally possess a high triplet quantum yield leading to the substantial production of $^1\text{O}_2$ upon irradiation. The research on PS should also comprehensively consider their photophysical properties, biocompatibility, targeting, and metabolic pathways to ensure the safety and efficacy of clinical PDT application. It should also be noted that PDT is less effective in hypoxia conditions, since $^1\text{O}_2$ generation in the PDT process requires oxygen and the process also consumes oxygen; therefore, PDT effectiveness can be directly affected by the tissue oxygen partial pressure and oxygenation status. Since the severity of PDT-induced photocytotoxicity is governed by the temporal and spatial distribution of $^1\text{O}_2$, the overproduction of $^1\text{O}_2$ in normal tissue during PDT treatment could cause unwanted collateral damage and side effects.

However, due to the technique difficulty in the direct detection of $^1\text{O}_2$ and the implementation of $^1\text{O}_2$ dosimetry, quantifying the in vivo production of $^1\text{O}_2$ is often an overlooked factor in PS evaluation and PDT dosimetry. In clinical practice, the λ_{max} , \mathcal{E}_{max} , and Φ_{Δ} of PS can be used as the main criteria for selecting a particular PS. The Φ_{Δ} is often used for the evaluation of the ability of a PS to produce $^1\text{O}_2$. It should be noted that, as described above, the reported Φ_{Δ} values of regulatory-approved PS are often determined in organic solvents. Even measured under the same condition, the Φ_{Δ} for the same PS may differ by measurement methods. Although the direct detection of $^1\text{O}_2$ and Φ_{Δ} is more technically challenging within biological environments and particularly in clinical setup, the quantitative techniques for $^1\text{O}_2$ measurement during photosensitization are of immense importance of values for both preclinical and clinical evaluation of potential PSs for future clinical use, for example, the direct singlet oxygen luminescence dosimetry (SOLD). In the scenarios where direct $^1\text{O}_2$ luminescence detection is difficult, the macroscopic singlet oxygen explicit dosimetry (SOED), which involves the measurement of the key components in the PDT photosensitizer concentration, ground-state oxygen concentration ($[\text{}^3\text{O}_2]$), and light fluence to calculate the amount of reacted $^1\text{O}_2$, might offer a viable alternative for quantifying $^1\text{O}_2$ in PDT.

Author Contributions: Conceptualization, S.C., X.G., Z.H. and T.C.Z.; draft preparation, S.C., X.G., S.W., Z.W. and D.H.; proofreading, X.Z., T.C.Z. and Z.H.; and typesetting, S.C., X.G., Z.W. and D.H. All authors have read and agreed to the published version of the manuscript.

Funding: This research and APC are funded in part by the National Natural Science Foundation of China (No. 81471703).

Conflicts of Interest: The authors declare no conflicts of interest.

References

1. Patrizia, A.; Kristian, B.; Keith, A.C.; Thomas, H.F.; Albert, W.G.; Sandra, O.G.; Stephen, M.H.; Michael, R.H.; Asta, J.; David, K.; et al. Photodynamic Therapy of Cancer: An Update. *CA Cancer J. Clin.* **2011**, *61*, 250–281.
2. Kamanli, A.F.; Çetinel, G.; Yıldız, M.Z. A New Handheld Singlet Oxygen Detection System (SODS) and NIR Light Source Based Phantom Environment for Photodynamic Therapy Applications. *Photodiagnosis Photodyn. Ther.* **2020**, *29*, 101577. [[CrossRef](#)] [[PubMed](#)]
3. Allison, R.R.; Huang, Z.; Dallimore, I.; Moghissi, K. Tools of Clinical Photodynamic Therapy (PDT): A Mini Compendium. *Photodiagnosis Photodyn. Ther.* **2024**, *46*, 104058. [[CrossRef](#)]
4. Kwiatkowski, S.; Knap, B.; Przystupski, D.; Saczko, J.; Kędzierska, E.; Knap-Czop, K.; Kotlińska, J.; Michel, O.; Kotowski, K.; Kulbacka, J. Photodynamic Therapy—Mechanisms, Photosensitizers and Combinations. *Biomed. Pharmacother.* **2018**, *106*, 1098–1107. [[CrossRef](#)]
5. Pustimbara, A.; Li, C.; Ogura, S.I. Hemin Enhance s the 5-aminolevulinic Acid-Photodynamic Therapy Effect Through the Changes of Cellular Iron Homeostasis. *Photodiagnosis Photodyn. Ther.* **2024**, *48*, 104253. [[CrossRef](#)]
6. Pierre, G.; Jean-François, S.; Georges, W.; Mizeret, J.; Woodtli, A.; Jean-François, T.; Fontolliet, C.; Hubert, V.; Ph, M. Tetra(m-hydroxyphenyl)chlorin Clinical Photodynamic Therapy of Early Bronchial and Oesophageal Cancers. *Laser Med. Sci.* **1996**, *11*, 227–235.
7. David, K. Pharmacokinetics of N-aspartyl Chlorin e6 in Cancer Patients. *J. Photochem. Photobiol. B* **1997**, *39*, 81–83.
8. Ming, L.; Changhua, L. Recent Advances in Activatable Organic Photosensitizers for Specific Photodynamic Therapy. *ChemPlusChem* **2020**, *85*, 948–957.
9. Ochsner, M. Photophysical and Photobiological Processes in the Photodynamic Therapy of Tumours. *J. Photochem. Photobiol. B* **1997**, *39*, 1–18. [[CrossRef](#)]
10. Castano, A.P.; Demidova, T.N.; Hamblin, M.R. Mechanisms in Photodynamic Therapy: Part Two-Cellular Signaling, Cell Metabolism and Modes of Cell Death. *Photodiagnosis Photodyn. Ther.* **2005**, *2*, 1–23. [[CrossRef](#)]
11. Weishaupt, K.R.; Gomer, C.J.; Dougherty, T.J. Identification of Singlet Oxygen as the Cytotoxic Agent in Photoinactivation of a Murine Tumor. *Cancer Res.* **1976**, *36*, 2326–2329. [[PubMed](#)]
12. Murotomi, K.; Umeno, A.; Shichiri, M.; Tanito, M.; Yoshida, Y. Significance of Singlet Oxygen Molecule in Pathologies. *Int. J. Mol. Sci.* **2023**, *24*, 2739. [[CrossRef](#)]
13. DeRosa, M.C.; Crutchley, R.J. Photosensitized Singlet Oxygen and its Applications. *Coord. Chem. Rev.* **2002**, *233–234*, 351–371. [[CrossRef](#)]
14. Foote, C.S. Mechanisms of Photosensitized Oxidation. There are Several Different Types of Photosensitized Oxidation Which May be Important in Biological Systems. *Science* **1968**, *162*, 963–970. [[CrossRef](#)] [[PubMed](#)]
15. Salokhiddinov, K.I.; Dzhangarov, B.M.; Byteva, I.M.; Gurinovich, G.P. Photosensitized Luminescence of Singlet Oxygen in Solutions at 1588 nm. *Chem. Phys. Lett.* **1980**, *76*, 85–87. [[CrossRef](#)]
16. Macpherson, A.N.; Truscott, T.G.; Turner, P.H. Fourier-Transform Luminescence Spectroscopy of Solvated Singlet Oxygen. *J. Chem. Soc. Faraday Trans.* **1994**, *90*, 1065–1072. [[CrossRef](#)]
17. Spiller, W.; Kliesch, H.; Wöhrle, D.; Hackbarth, S.; Röder, B.; Schnurpfeil, G. Singlet Oxygen Quantum Yields of Different Photosensitizers in Polar Solvents and Micellar Solutions. *J. Porphyr. Phthalocya* **1998**, *2*, 145–158. [[CrossRef](#)]
18. Darwent, J.R.; Douglas, P.; Harriman, A.; Porter, G.; Richoux, M.C. Metal Phthalocyanines and Porphyrins as Photosensitizers for Reduction of Water to Hydrogen. *Coord. Chem. Rev.* **1982**, *44*, 83–126. [[CrossRef](#)]
19. Gunduz, H.; Kolemen, S.; Akkaya, E.U. Singlet Oxygen Probes: Diversity in Signal Generation Mechanisms Yields a Larger Color Palette. *Coord. Chem. Rev.* **2021**, *429*, 213641. [[CrossRef](#)]
20. Losev, A.P.; Nichiporovich, I.N.; Byteva, I.M.; Drozdov, N.N.; Jghgami, I.F.A. The Perturbing Effect of Solvents on the Luminescence Rate Constant of Singlet Molecular Oxygen. *Chem. Phys. Lett.* **1991**, *181*, 45–50. [[CrossRef](#)]
21. Kearns, D.R. Physical and Chemical Properties of Singlet Molecular Oxygen. *Chem. Rev.* **1971**, *71*, 395–427. [[CrossRef](#)]
22. Kramarenko, G.G.; Hummel, S.G.; Martin, S.M.; Buettner, G.R. Ascorbate Reacts with Singlet Oxygen to Produce Hydrogen Peroxide. *Photochem. Photobiol.* **2006**, *82*, 1634–1637. [[CrossRef](#)] [[PubMed](#)]
23. Schweitzer, C.; Schmidt, R. Physical Mechanisms of Generation and Deactivation of Singlet Oxygen. *Chem. Rev.* **2003**, *103*, 1685–1757. [[CrossRef](#)] [[PubMed](#)]
24. Gollnick, K.; Schenck, G.O. Mechanism and Stereoselectivity of Photosensitized Oxygen Transfer Reactions. *Pure Appl. Chem.* **1964**, *9*, 507–526. [[CrossRef](#)]
25. Foote, C.S.; Denny, R.W. Chemistry of Singlet Oxygen. VII. Quenching by Beta.-Carotene. *J. Am. Chem. Soc.* **1968**, *90*, 6233–6235. [[CrossRef](#)]
26. Hall, R.D.; Chignell, C.F. Steady-State Near-Infrared Detection of Singlet Molecular Oxygen: A Stern-Volmer Quenching Experiment with Sodium Azide. *Photochem. Photobiol.* **1987**, *45*, 459–464. [[CrossRef](#)]
27. Gorman, A.A.; Ian, R.G.; Hamblett, I.; Standen, M.C. Reversible Exciplex Formation Between Singlet Oxygen, 1.DELTA.g, and Vitamin E. Solvent and Temperature Effects. *J. Am. Chem. Soc.* **1984**, *106*, 6956–6959. [[CrossRef](#)]

28. Michaeli, A.; Feitelson, J. Reactivity of Singlet Oxygen Toward Amino Acids and Peptides. *Photochem. Photobiol.* **1994**, *59*, 284–289. [[CrossRef](#)] [[PubMed](#)]
29. Matheson, I.B.; Etheridge, R.D.; Kratowich, N.R.; Lee, J. The Quenching of Singlet Oxygen by Amino Acids and Proteins. *Photochem. Photobiol.* **1975**, *21*, 165–171. [[CrossRef](#)]
30. Di Mascio, P.; Martinez, G.R.; Miyamoto, S.; Ronsein, G.E.; Medeiros, M.H.G.; Cadet, J. Singlet Molecular Oxygen Reactions with Nucleic Acids, Lipids, and Proteins. *Chem. Rev.* **2019**, *119*, 2043–2086. [[CrossRef](#)]
31. Moan, J. On the Diffusion Length of Singlet Oxygen in Cells and Tissues. *J. Photochem.* **1990**, *6*, 343–344. [[CrossRef](#)]
32. Ethirajan, M.; Chen, Y.; Joshi, P.; Pandey, R.K. The Role of Porphyrin Chemistry in Tumor Imaging and Photodynamic Therapy. *Chem. Soc. Rev.* **2011**, *40*, 340–362. [[CrossRef](#)] [[PubMed](#)]
33. Klaper, M.; Linker, T. New Singlet Oxygen Donors Based on Naphthalenes: Synthesis, Physical Chemical Data, and Improved Stability. *Chemistry* **2015**, *21*, 8569–8577. [[CrossRef](#)]
34. Winterbourn, C.C. Reconciling the Chemistry and Biology of Reactive Oxygen Species. *Nat. Chem. Biol.* **2008**, *4*, 278–286. [[CrossRef](#)] [[PubMed](#)]
35. Grune, T.; Schröder, P.; Biesalski, H.K. Low Molecular Weight Antioxidants. In *Reactions, Processes: Oxidants and Antioxidant Defense Systems*; Grune, T., Ed.; Springer Berlin Heidelberg: Berlin/Heidelberg, Germany, 2005; pp. 77–90.
36. Kruk, J.; Szymańska, R. Singlet Oxygen Oxidation Products of Carotenoids, Fatty Acids and Phenolic Prenylipids. *J. Photochem. Photobiol. B* **2021**, *216*, 112148. [[CrossRef](#)]
37. Kim, J.; Rodriguez, M.E.; Guo, M.; Kenney, M.E.; Oleinick, N.L.; Anderson, V.E. Oxidative Modification of Cytochrome c by Singlet Oxygen. *Free Radic. Biol. Med.* **2008**, *44*, 1700–1711. [[CrossRef](#)]
38. Marques, E.F.; Medeiros, M.H.G.; Di Mascio, P. Lysozyme Oxidation by Singlet Molecular Oxygen: Peptide Characterization Using ^{18}O -Labeling Oxygen and nLC-MS/MS. *J. Mass. Spectrom.* **2017**, *52*, 739–751. [[CrossRef](#)]
39. Yin, H.; Xu, L.; Porter, N.A. Free Radical Lipid Peroxidation: Mechanisms and Analysis. *Chem. Rev.* **2011**, *111*, 5944–5972. [[CrossRef](#)]
40. Rougee, M.; Bensasson, R.V.; Land, E.J.; Pariente, R. Deactivation of Singlet Molecular Oxygen by Thiols and Related Compounds, Possible Protectors Against Skin Photosensitivity. *Photochem. Photobiol.* **1988**, *47*, 485–489. [[CrossRef](#)]
41. Cadet, J.; Davies, K.J.A.; Medeiros, M.H.; Di Mascio, P.; Wagner, J.R. Formation and Repair of Oxidatively Generated Damage in Cellular DNA. *Free Radic. Biol. Med.* **2017**, *107*, 13–34. [[CrossRef](#)]
42. Liu, Y.; Yu, X.; Kamali, M.; Zhang, X.; Feijoo, S.; Al-Salem, S.M.; Dewil, R.; Appels, L. Biochar in Hydroxyl Radical-Based Electrochemical Advanced Oxidation Processes (eAOPs)—Mechanisms and Prospects. *Chem. Eng. J.* **2023**, *467*, 143291. [[CrossRef](#)]
43. Gulcin, İ. Antioxidants and Antioxidant Methods: An Updated Overview. *Arch. Toxicol.* **2020**, *94*, 651–715. [[CrossRef](#)]
44. Halliwell, B.; Gutteridge, J.M.C. *Free Radicals in Biology and Medicine*; Oxford University Press: Oxford, UK, 2015.
45. Sies, H. Oxidative Stress: Oxidants and Antioxidants. *Exp. Physiol.* **1997**, *82*, 291–295. [[CrossRef](#)] [[PubMed](#)]
46. Huang, D.; Ou, B.; Prior, R.L. The Chemistry Behind Antioxidant Capacity Assays. *J. Agric. Food Chem.* **2005**, *53*, 1841–1856. [[CrossRef](#)] [[PubMed](#)]
47. Vani, R.; Masannagari, P.; Aastha, C.; Chaitra, B.; Prerana, B.; Ranjithvishal; Shruthi, L.; Sudharshan, N. Reactive Oxygen Species and Antioxidant Interactions in Erythrocytes. In *The Erythrocyte*; Vani, R., Ed.; IntechOpen: Rijeka, Croatia, 2022; Chapter 1.
48. Zhang, H.; Limphong, P.; Pieper, J.; Liu, Q.; Rodesch, C.K.; Christians, E.; Benjamin, I.J. Glutathione-Dependent Reductive Stress Triggers Mitochondrial Oxidation and Cytotoxicity. *FASEB J.* **2012**, *26*, 1442–1451. [[CrossRef](#)]
49. Fujii, J.; Soma, Y.; Matsuda, Y. Biological Action of Singlet Molecular Oxygen from the Standpoint of Cell Signaling, Injury and Death. *Molecules* **2023**, *28*, 4085. [[CrossRef](#)]
50. Huang, Z.; Xu, H.; Meyers, A.D.; Musani, A.I.; Wang, L.; Tagg, R.; Barqawi, A.B.; Chen, Y.K. Photodynamic Therapy for Treatment of Solid Tumors—Potential and Technical Challenges. *Technol. Cancer Res. Treat.* **2008**, *7*, 309–320. [[CrossRef](#)]
51. Uzdensky, A.B.; Berezhnaya, E.; Kovaleva, V.; Neginskaya, M.; Rudkovskii, M.; Sharifulina, S. Photodynamic Therapy: A Review of Applications in Neurooncology and Neuropathology. *J. Biomed. Opt.* **2015**, *20*, 61108. [[CrossRef](#)]
52. Yang, W.; Rastogi, V.; Sun, H.; Sharma, D.; Wilson, B.C.; Hadfield, R.H.; Zhu, T.C. Multispectral Singlet Oxygen Luminescent Dosimetry (MSOLD) for Photofrin-mediated Photodynamic Therapy. *Proc. SPIE Int. Soc. Opt. Eng.* **2023**, *12359*, 1235908.
53. Li, B.; Shen, Y.; Lin, H.; Wilson, B.C. Correlation of in Vitro Cell Viability and Cumulative Singlet Oxygen Luminescence from Protoporphyrin IX in Mitochondria and Plasma Membrane. *Photodiagnosis Photodyn. Ther.* **2024**, *46*, 104080. [[CrossRef](#)]
54. Gemmell, N.R.; McCarthy, A.; Kim, M.M.; Veilleux, I.; Zhu, T.C.; Buller, G.S.; Wilson, B.C.; Hadfield, R.H. A Compact Fiber-Optic Probe-Based Singlet Oxygen Luminescence Detection System. *J. Biophotonics* **2017**, *10*, 320–326. [[CrossRef](#)] [[PubMed](#)]
55. Gemmell, N.R.; McCarthy, A.; Liu, B.; Tanner, M.G.; Dorenbos, S.D.; Zwiller, V.; Patterson, M.S.; Buller, G.S.; Wilson, B.C.; Hadfield, R.H. Singlet Oxygen Luminescence Detection with a Fiber-Coupled Superconducting Nanowire Single-Photon Detector. *Opt. Express* **2013**, *21*, 5005–5013. [[CrossRef](#)]
56. Cui, S.; Ke, C.; Peng, W.; You, L.; Zhang, X.; Huang, Z. Optimizing Single Photon Detection Based on Superconducting Strip Photon Detector (SSPD) for Singlet Oxygen Luminescence Detection. *Proc. SPIE* **2023**, *12770*, 127702S1–127702S8.
57. McIntosh, A.R.; Bolton, J.R. Triplet State Involvement in Primary Photochemistry of Photosynthetic Photosystem II. *Nature* **1976**, *263*, 443–445. [[CrossRef](#)]
58. Nishide, N.; Miyoshi, N. Singlet Oxygen Trapping by DRD156 in Micellar Solutions. *Life Sci.* **2002**, *72*, 321–328. [[CrossRef](#)]

59. Gomes, A.; Fernandes, E.; Lima, J.L. Fluorescence Probes Used for Detection of Reactive Oxygen Species. *J. Biochem. Biophys. Methods* **2005**, *65*, 45–80. [\[CrossRef\]](#) [\[PubMed\]](#)
60. Song, D.; Cho, S.; Han, Y.; You, Y.; Nam, W. Ratiometric Fluorescent Probes for Detection of Intracellular Singlet Oxygen. *Org. Lett.* **2013**, *15*, 3582–3585. [\[CrossRef\]](#)
61. Umezawa, N.; Tanaka, K.; Urano, Y.; Kikuchi, K.; Higuchi, T.; Nagano, T. Novel Fluorescent Probes for Singlet Oxygen. *Angew. Chem. Int. Ed. Engl.* **1999**, *38*, 2899–2901. [\[CrossRef\]](#)
62. Tanaka, K.; Miura, T.; Umezawa, N.; Urano, Y.; Kikuchi, K.; Higuchi, T.; Nagano, T. Rational Design of Fluorescein-Based Fluorescence Probes. Mechanism-Based Design of a Maximum Fluorescence Probe for Singlet Oxygen. *J. Am. Chem. Soc.* **2001**, *123*, 2530–2536. [\[CrossRef\]](#)
63. Arnab, M. Photophysical Detection of Singlet Oxygen. In *Reactive Oxygen Species*; Ahmad, R., Surguchov, A., Eds.; IntechOpen: London, UK, 2022; Chapter 2; pp. 1–20. 2022.
64. Ragàs, X.; Jiménez-Banzo, A.; Sánchez-García, D.; Batllori, X.; Nonell, S. Singlet Oxygen Photosensitisation by the Fluorescent Probe Singlet Oxygen Sensor Green. *Chem Commun (Camb)* **2009**, *20*, 2920–2922. [\[CrossRef\]](#)
65. Murotomi, K.; Umeno, A.; Sugino, S.; Yoshida, Y. Quantitative Kinetics of Intracellular Singlet Oxygen Generation Using a Fluorescence Probe. *Sci. Rep.* **2020**, *10*, 10616. [\[CrossRef\]](#) [\[PubMed\]](#)
66. Lindig, B.A.; Rodgers, M.A.J.; Schaap, A.P. Determination of the Lifetime of Singlet Oxygen in Water-d₂ Using 9,10-anthracenedipropionic Acid, a Water-Soluble Probe. *J. Am. Chem. Soc.* **1980**, *102*, 5590–5593. [\[CrossRef\]](#)
67. Song, B.; Wang, G.; Yuan, J. Measurement and Characterization of Singlet Oxygen Production in Copper ion-Catalyzed Aerobic Oxidation of Ascorbic Acid. *Talanta* **2007**, *72*, 231–236. [\[CrossRef\]](#) [\[PubMed\]](#)
68. Moreno, M.J.; Monson, E.; Reddy, R.G.; Rehemtulla, A.; Ross, B.D.; Philbert, M.; Schneider, R.J.; Kopelman, R. Production of Singlet Oxygen by Ru(dpp(SO₃)₂)₃ Incorporated in Polyacrylamide PEBBLES. *Sens. Actuat B-Chem.* **2003**, *90*, 82–89. [\[CrossRef\]](#)
69. Yasuta, N.; Takenaka, N.; Takemura, T. Mechanism of Photosensitized Chemiluminescence of 2-Methyl-6-phenylimidazo[1,2-a]pyrazin-3(7H)-one (CLA) in Aqueous Solution. *Chem. Lett.* **2003**, *28*, 451–452. [\[CrossRef\]](#)
70. Li, X.; Zhang, G.; Ma, H.; Zhang, D.; Li, J.; Zhu, D. 4,5-Dimethylthio-4'-[2-(9-anthryloxy)ethylthio]tetraethiafulvalene, a Highly Selective and Sensitive Chemiluminescence Probe for Singlet Oxygen. *J. Am. Chem. Soc.* **2004**, *126*, 11543–11548. [\[CrossRef\]](#)
71. Bresolí-Obach, R.; Torra, J.; Zanolto, R.P.; Zanolto, A.L.; Nonell, S. Singlet Oxygen Quantum Yield Determination Using Chemical Acceptors. *Methods Mol. Biol.* **2021**, *2202*, 165–188.
72. Tanielian, C.; Wolff, C.; Esch, M. Singlet Oxygen Production in Water: Aggregation and Charge-Transfer Effects. *J. Phys. Chem.* **1996**, *100*, 6555–6560. [\[CrossRef\]](#)
73. Fernandez, J.M.; Bilgin, M.D.; Grossweiner, L.I. Singlet Oxygen Generation by Photodynamic Agents. *J. Photochem. Photobiol. B* **1997**, *37*, 131–140. [\[CrossRef\]](#)
74. Hadjur, C.; Wagnieres, G.; Monnier, P.; van den Bergh, H. EPR and Spectrophotometric Studies of Free Radicals (O₂^{•−}, •OH, BPD-MA) and Singlet Oxygen (¹O₂) Generated by Irradiation of Benzoporphyrin Derivative Monoacid Ring A. *Photochem. Photobiol.* **1997**, *65*, 818–827. [\[CrossRef\]](#)
75. Nishimura, T.; Hara, K.; Honda, N.; Okazaki, S.; Hazama, H.; Awazu, K. Determination and Analysis of Singlet Oxygen Quantum Yields of Talaporfin Sodium, Protoporphyrin IX, and Lipidated Protoporphyrin IX Using Near-Infrared Luminescence Spectroscopy. *Lasers Med. Sci.* **2020**, *35*, 1289–1297. [\[CrossRef\]](#) [\[PubMed\]](#)
76. Bregnhøj, M.; Thorning, F.; Ogilby, P.R. Singlet Oxygen Photophysics: From Liquid Solvents to Mammalian Cells. *Chem. Rev.* **2024**, in press. [\[CrossRef\]](#)
77. Tanielian, C.; Schweitzer, C.; Mechin, R.; Wolff, C. Quantum Yield of Singlet Oxygen Production by Monomeric and Aggregated Forms of Hematoporphyrin Derivative. *Free Radical Biol. Med.* **2001**, *30*, 208–212. [\[CrossRef\]](#) [\[PubMed\]](#)
78. Bautista-Sanchez, A.; Kasselouri, A.; Desroches, M.C.; Blais, J.; Maillard, P.; de Oliveira, D.M.; Tedesco, A.C.; Prognon, P.; Delaire, J. Photophysical Properties of Glucoconjugated Chlorins and Porphyrins and their Associations with Cyclodextrins. *J. Photochem. Photobiol. B* **2005**, *81*, 154–162. [\[CrossRef\]](#)
79. Spikes, J.D.; Bommer, J.C. Photosensitizing Properties of Mono-L-Aspartyl Chlorin e6 (NPe6): A Candidate Sensitizer for the Photodynamic Therapy of Tumors. *J. Photochem. Photobiol. B* **1993**, *17*, 135–143. [\[CrossRef\]](#) [\[PubMed\]](#)
80. Aveline, B.; Hasan, T.; Redmond, R.W. Photophysical and Photosensitizing Properties of Benzoporphyrin Derivative Monoacid Ring A (BPD-MA)*. *Photochem. Photobiol.* **1994**, *59*, 328–335. [\[CrossRef\]](#) [\[PubMed\]](#)
81. Yoon, I.; Li, J.Z.; Shim, Y.K. Advance in Photosensitizers and Light Delivery for Photodynamic Therapy. *Clin. Endosc.* **2013**, *46*, 7–23. [\[CrossRef\]](#)
82. Przygoda, M.; Bartusik-Aebisher, D.; Dynarowicz, K.; Cieślak, G.; Kawczyk-Krupka, A.; Aebisher, D. Cellular Mechanisms of Singlet Oxygen in Photodynamic Therapy. *Int. J. Mol. Sci.* **2023**, *24*, 16890. [\[CrossRef\]](#)
83. Hu, W.; Zhang, R.; Zhang, X.F.; Liu, J.; Luo, L. Halogenated BODIPY Photosensitizers: Photophysical Processes for Generation of Excited Triplet State, Excited Singlet State and Singlet Oxygen. *Spectrochim. Acta A Mol. Biomol. Spectrosc.* **2022**, *272*, 120965. [\[CrossRef\]](#)
84. Li, N.; Cui, S.; Yang, A.; Xiao, B.; Cao, Y.; Yang, X.; Lin, C. Sequence-Dependent Effects of Hematoporphyrin Derivatives (HPD) Photodynamic Therapy and Cisplatin on Lung Adenocarcinoma Cells. *Photodiagnosis Photodyn. Ther.* **2024**, *47*, 104102. [\[CrossRef\]](#)
85. Wang, S.; Bromley, E.; Xu, L.; Chen, J.C.; Keltner, L. Talaporfin sodium. *Expert. Opin. Pharmacother.* **2010**, *11*, 133–140. [\[CrossRef\]](#) [\[PubMed\]](#)

86. Zheng, B.D.; He, Q.X.; Li, X.; Yoon, J.; Huang, J.D. Phthalocyanines as Contrast Agents for Photothermal Therapy. *Coord. Chem. Rev.* **2021**, *426*, 213548. [[CrossRef](#)]
87. Hurley, D.J.; Gallagher, D.; Petronzi, V.; O'Rourke, M.; Kinsella, F.; Townley, D. Examining the Efficacy of Verteporfin Photodynamic Therapy (PDT) at Different Dose & Fluence Levels. *Photodiagnosis Photodyn. Ther.* **2023**, *44*, 103848. [[PubMed](#)]
88. Pihl, C.; Lerche, C.M.; Andersen, F.; Bjerring, P.; Haedersdal, M. Improving the Efficacy of Photodynamic Therapy for Actinic Keratosis: A Comprehensive Review of Pharmacological Pretreatment Strategies. *Photodiagnosis Photodyn. Ther.* **2023**, *43*, 103703. [[CrossRef](#)]

Disclaimer/Publisher's Note: The statements, opinions and data contained in all publications are solely those of the individual author(s) and contributor(s) and not of MDPI and/or the editor(s). MDPI and/or the editor(s) disclaim responsibility for any injury to people or property resulting from any ideas, methods, instructions or products referred to in the content.